

River plume fronts and their implications on the biological production of the Bay of Bengal, Indian Ocean

**Kusum Komal Karati^{a,b*}, Vineetha G^{a,c}, Raveendran TV^a, Muraleedharan KR^a,
Habeebrehman H^d, Philson KP^a, Achuthankutty CT^a**

a- CSIR-National Institute of Oceanography, Regional Center, Kochi, India. Postal Code: 682018

b- Centre for Marine Living Resources and Ecology, Kochi, India, Postal code: 682037

c- Central Marine Fisheries Research Institute, Kochi, India, Postal code: 682018

d - Calicut University, Kerala, India. Postal Code: 673632

*Corresponding author: Kusum Komal Karati,

Centre for Marine Living Resources and Ecology, Kochi, India, Postal code: 682037

Phone number: 91 9895305666, E mail address – kusum.kk1@gmail.com

Abstract:

Fronts are the physical interface between water masses of distinct hydrographic characteristics and are ubiquitous features of the Bay of Bengal (BoB). They form as a result of receiving high freshwater runoff from many large rivers, but the biological characteristics are mostly unexamined. We determined the distribution of fronts in the BoB during the fall intermonsoon period and examined the physicochemical couplings in the frontal regions and their concomitant effect on biological production. The *in situ* sea surface salinity (SSS) gradients were used to delineate the fronts (threshold of 0.01 psu / km), and two frontal zones with a cross-frontal SSS difference of 1 – 3 psu were identified. River discharge was found to have a more significant role than direct precipitation in the frontogenesis of this ecosystem. These narrow three-dimensional boundaries were characterized by a higher nutrient replenishment than in the contiguous non-front zones, and had a higher phytoplankton production. The highest accumulation of zooplankton biomass in the intermediate saline water masses (31-33 psu) of the frontal regions was the subsequent effect of the higher food availability and congregation by the hydrodynamic convergences.

Keywords: River plume fronts; Bay of Bengal; Chlorophyll *a*; Primary production; Zooplankton

Introduction

Fronts, the dynamic borderline between water masses of distinct hydrographic characteristics, are ubiquitous features of oceanic regions (Lentz & Limeburber 1995, Bakun 2006, Belkin et al. 2009). The driving forces behind the genesis of these narrow three-dimensional natural boundaries vary and range from current convergence, coastal upwelling, continental runoff, differential solar heating to changes in the bathymetry (Franks 1992, Acha et al. 2015). As a zone where laterally convergent flows induce and intensify the vertical flow, the frontal regions experience nutrient replenishment of the surface waters (Owen 1981). This results in enhanced primary production, which in turn gets channeled to higher trophic levels in the pelagic food web (Laubscher et al. 1993, Lohrenz et al. 1999). Thus, the subsequent aggregation of the biotic communities in the frontal areas delineates them as one of the prominent pelagic foraging hotspots in the oligotrophic tropical oceanic regions (Scales et al. 2014). There are comprehensive studies on fronts and their ecological significance in the Pacific and the Atlantic Oceans (Lohrenz et al. 1999, Belkin & Cornillon 2003, and reference thereafter, Albania & Irigoien 2004), but information on the occurrence, forcing mechanisms, and also the influence of fronts on the biological production is scarce from the northern Indian Ocean. The information on fronts there is mostly limited to the thermal fronts of the Arabian Sea in the western half of the northern Indian Ocean (Evans & Brown 1981, Sarma et al. 2015, Vipin et al. 2015).

The Bay of Bengal (BoB) in the eastern half of the northern Indian Ocean, was traditionally considered as a less productive ocean basin compared to its western counterpart, the Arabian Sea, owing to the weak wind patterns and intense freshwater influenced vertical stratification (Qasim 1977, Prasanna Kumar et al. 2002). However, in the recent years, many oceanographic researches conducted in the BoB indicated an enhanced biological productivity in the BoB influenced by physical processes like eddy and cyclones (Madhu et al. 2002, Prasanna Kumar et al. 2004, 2007, Fernandes & Ramaiah 2013, Singh & Ramesh 2015, Singh et al. 2015) (see Table 1 for details). In contrast to the Arabian Sea, the BoB receives a heavy runoff ($1.6 \times 10^{12} \text{ m}^3 \text{ yr}^{-1}$) from many large perennial rivers like the Ganges, Brahmaputra, Irrawaddy, Godavari, Krishna and Kaveri and their tributaries (Subramanian 1993). These large river discharges in the north result in the formation of freshwater plumes which move equatorward against local winds because of the interaction of lighter surface water, heavier saline water, and the coast, and develop a frontal structure with an across front salinity difference of 1 psu (Shetye et al. 1991). The prominent north-south gradient of the sea surface salinity (SSS) in the Levitus climatology also fortifies the view (Fig. 1a). Based on the mixed layer salt budget investigation, it has been observed that both river discharge and precipitation

contribute to the SSS variability and gradient in the BoB (Chaitanya et al. 2015). Furthermore, the strength and the direction of the flow of East Indian Coastal Current (EICC) is also known to have a crucial role in the advection of the freshwater plume in the BoB (Akhil et al. 2014, Chaitanya et al. 2014). The dynamics of the EICC is controlled by many forcing mechanisms like local alongshore winds, interior Ekman pumping, remote alongshore winds adjacent to the eastern boundaries of the bay, and remotely forced signals of the Kelvin waves propagating from the equator (McCreary et al. 1996). Any variations in these factors influence the EICC and, in turn, generates spatiotemporal variation in the structure of the salinity front in the BoB. Hence, while investigating the salinity fronts and their influence on the biotic community in BoB, the study of the significance of freshwater discharges, precipitation, and the EICC to frontogenesis gains importance.

There is a paucity of knowledge on the existence of fronts and their implications on the production of BoB. Hence, this study aims to: (1) identify the salinity fronts in the BoB; and (2) evaluate their influence on the plankton community. As a pioneering attempt addressing the influence of oceanic fronts on the plankton community of the BoB, the results will be helpful to better understand the processes modulating the biological production of this significant part of the northern Indian Ocean.

Material And Methods

Sampling design

There is less spatial variability in the sea surface temperature in the BoB than in sea surface salinity which is often pronounced in the north-south direction (Levitus 1982, Akhil et al. 2014). The SSS of the region was plotted on a monthly scale, based on the climatological data of the North Indian Ocean Atlas ([www.nio.org/index/option/com_nomenu/task/show/](http://www.nio.org/index/option/com_nomenu/task/show/tid/2/sid/18/id/229)

[tid/2/sid/18/id/229](http://www.nio.org/index/option/com_nomenu/task/show/tid/2/sid/18/id/229)). This climatological atlas encompasses the data sets of the World Ocean Atlas (Antonov et al. 2010) and information generated by various research organizations of India, and so it is considered as a reliable ocean atlas of this region (Chatterjee et al. 2012). We used the data to choose sampling dates on one cruise during the late summer monsoon to fall intermonsoon period (September – October 2006) when the north-south gradient in salinity was high because of the influence of the freshwater plume (Fig. 1 b,c). Additionally, to identify whether the *in situ* salinity distribution of the present study period was a representative of the fall intermonsoon salinity distribution in the BoB, the satellite-based SSS data (Aquarius) of the respective months (September and October) were critically analyzed. Because the satellite SSS data is comparatively less available than the SST data, according to the accessibility of the Aquarius SSS data of the respective months, a detailed evaluation of data spanning a period of 3 years from 2012 -14 was incorporated into the

analysis (<https://oceanwatch.pifsc.noaa.gov>). The analysis of the monthly river discharges into the BoB was carried out based on the information acquired from Ismail (2011), which was estimated using the global river discharge data base and central water commission of India. The data were further cross-checked based on the information from Papa et al. (2012) and Chaitanya et al. (2014). The climatological precipitation data were prepared based on the monthly precipitation values from the Tropical Rainfall Measuring Mission (2001 to 2010).

Sampling locations ($n = 31$) were fixed along five zonal transects from 11° N to 19° N and the stations were distributed at intervals of 1° longitude (6-7 stations at a distance of ~ 110 km), extending from the coast to offshore (Fig. 2a). We identified the frontal zones in the Bay of Bengal and evaluated their influence on the plankton community. For understanding the diurnal changes in distribution, one coastal and one offshore station were monitored along each transect. The sampling was done at 6-hour intervals for 24 hours. The day and night sampling periods were determined based on the local time of sunrise/sunset.

Abiotic components

A SBE Seabird 911 plus CTD (accuracy of conductivity 0.0003 S/m, temperature 0.001°C , and pressure 0.015%) was deployed at each station to obtain the temperature and salinity profiles of the water column. The instrument was operated down to 5 m off the bottom at the shallow coastal stations and down to 1000 m depth at the offshore stations. The salinity values obtained from the CTD were calibrated against an Autosal (Guildline 8400) onboard to minimize the error factor in the salinity data sets. The potential density (σ_t) was computed from the pressure, temperature and salinity values obtained from the CTD. Water samples were collected using a CTD Rosette sampler fitted with pre-cleaned 1.8-l Teflon coated Go-Flo bottles (General Oceanics) deployed from standard depths down to 150 m (surface, 10, 20, 30, 50, 75, 100, 150 m). The surface water was collected between 0 and 2 m. The pH was determined using a pH-meter whereas the DO was analyzed using Winkler's method (Grasshoff 1983). Nutrients (nitrate, phosphate, and silicate) were analyzed immediately onboard following standard colorimetric techniques (Grasshoff 1983) using a Skalar Segmented Flow Auto Analyzer (Model SA-1050). The precision of the nutrient measurement was $\pm 0.15 \mu\text{mol N l}^{-1}$ for nitrate, $\pm 0.04 \mu\text{mol P l}^{-1}$ for phosphate, and $\pm 0.05 \mu\text{mol Si l}^{-1}$ for silicate, respectively.

Biotic components

Samples for the phytoplankton biomass (chlorophyll *a*) and primary production (PP) estimation were collected from the standard depths down to 120 m (surface, 10, 20, 50, 75, 100 and 120 m) according

to the JGOFS protocols (UNESCO 1994). For chlorophyll *a*, 1 L of water samples of each depth were filtered through GF/F filters (pore size 0.7 μm), extracted with 10 ml of 90 % acetone in dark and analyzed using a UV/Vis, Shimadzu spectrophotometer (Strickland & Parsons 1972). Also, the MODIS-Aqua satellite ocean color data were used to get a clear picture of the surface chlorophyll *a* distribution of the study region ([www.http://gdata1.sci.gsfc.nasa.gov](http://gdata1.sci.gsfc.nasa.gov)). The PP was measured at one coastal station and one offshore station in each transect (the 10 diurnal stations). For the estimation of PP, water samples were collected just before the sunrise and were immediately passed through 200 μm plankton net to remove large sized zooplankton. Then they were transferred into five 300 ml (3 light and 2 dark) polycarbonate bottles for each depth (Nalgene–Germany). One ml of $\text{NaH}^{14}\text{CO}_3$ (specific activity 5 μCi) was added to all samples. The sample bottles were incubated *in situ* at the respective sampling depths for 12 h with the help of a mooring system. After the *in situ* incubation, bottles were retrieved and the water samples were filtered through 47-mm GF/F filters (pore size 0.7 μm) under gentle suction. The filters were exposed to concentrated HCl fumes (11.3 N) to remove the excess inorganic carbon and were subsequently stored in scintillation vials. One day before the analysis, 5 ml of liquid scintillation cocktail-T was added to each vial, and the radioactivity was measured in a scintillation counter (Wallac 1409 DSA Perkin Elmer, USA). The decays per minute (DPMs) values were converted into daily production rates ($\text{mg C m}^{-3} \text{ day}^{-1}$) following the standard methodology described in the JGOFS protocols (UNESCO 1994). The depthwise distribution of chlorophyll *a* and PP was integrated to obtain the phytoplankton biomass and production of the water column following Dyson et al. 1965 as:

$$\text{Column chlorophyll } a/\text{PP} = [(d_1 - d_0)(a_0 + a_1)/2 + (d_2 - d_1)(a_1 + a_2)/2 + \dots \dots \dots]$$

where, d_0, d_1, d_2 are the depths sampled; a_0, a_1, a_2 are the chlorophyll *a*/PP of the respective depths,

Sampling in shallow coastal stations was possible only down to a depth of 75 m. The integrated chlorophyll *a* and PP were thus calculated only for the 75 m water column for the spatial comparison.

Mesozooplankton sampling was carried out from two discrete depth zones viz. the mixed layer depth (MLD) and the thermocline (TC). The MLD was determined as the depth where density increases 0.2 kg m^{-3} from the surface value (Shetye et al. 1996), and the bottom of the TC was taken as the depth where the temperature reached 15°C . Sampling was carried out by vertical hauling (1 m sec^{-1}) of the multiple plankton net (Hydrobios, Germany), which works based on the principle of the opening and closing of a series of the individual plankton nets in succession at the desired depths. The mesh size of the net was 200 μm , and the opening and closing of the nets (mouth area 0.25 m^2)

at the prefixed depth zones were controlled by shipboard electronic sensors. The advantage of this net is the negligible rate of contamination among the samples along the depth layers (Weikert & John 1981). Zooplankton samples were then passed through a 200- μm mesh, and the excess water was removed with absorbent paper. The displacement volume method was followed for estimation of the mesozooplankton biomass, and expressed as ml m^{-3} (Harris et al. 2000). Different taxa of zooplankton were sorted, enumerated under a stereo-zoom microscope, and their corresponding abundance was calculated based on the volume of water filtered through the net and expressed as ind. m^{-3} . The mesozooplankton samples were collected from two discrete depth layers, and the consolidated abundance of the zooplankton community from the entire sampled depth was estimated according to the methods of Kusum et al. (2014a) as

$$X_{\text{consolidated}} = \sum_{i=1}^n \frac{Z_i X_i}{Z_i}$$

where X_i = biomass / abundance zooplankton at a particular stratum in a sampling location,

Z_i = depth of the particular stratum in a sampling location.

Data analyses

Correlation analysis

The CTD based *in situ* SSS value was correlated with the climatological data of the North Indian Ocean Atlas to assess its representability for the study area. Because the study was conducted during the month of September and October, the climatological data of the mean SSS of these two months were used for the analysis. The riverine influxes and precipitation are considered to have a significant role in the variability of SSS. Hence, a Pearson's correlation analysis was carried out based on the monthly climatological data of the respective variables to identify the interrelation existing between them and SSS using statistical software Graphpad prism (www.graphpad.com).

t-test and analysis of variance

The one-way analysis of variance (ANOVA) was carried out using the SSS data sets of both the satellite based information for 2012 to 2014 and the *in situ* data of the present study. The Bartlett's test for equal variances was used to assess the homogeneity of variances. The D'Agostino and Pearson omnibus normality test was performed before the analysis to check their normality in distribution. Based on the result of these statistical tests, either a parametric or non-parametric ANOVA (Kruskal-Wallis test) was performed for the variables with two-tailed P values and 95% confidence intervals. A t-test was carried out (two-tailed P values and 95% confidence intervals) between the frontal and non-frontal data of phytoplankton biomass, zooplankton biomass and

abundance to assess the significance in variation. In case of t-test also, the parametric and nonparametric analysis (Mann-Whitney test) was selected based on the normality test. The ANOVA and t-test were performed using Graphpad Prism. For all tests, we used the significance value, $\alpha = 0.05$.

Canonical Analysis of Principal Coordinates (CAP)

The constrained Canonical Analysis of Principal Coordinates (CAP) was performed (Andersons & Willis 2003) to understand the distinctness of the zooplankton community in the frontal zones from other locations. It was done based on the Bray-Curtis similarity index (Clifford & Stephensen 1975), and applied to the log-transformed data of the abundance of the zooplankton taxa using PRIMER (Clarke & Warwick 2001).

Multivariate dispersion analysis and analysis of similarities

The MVDISP algorithm was used to assess the variability in the zooplankton community structure of the frontal and non-frontal locations and to calculate the Index of Multivariate Dispersion (IMD). The analysis of similarity (one-way ANOSIM) was used to describe dissimilarities of the zooplankton community among the frontal and non-frontal regions. Both analyses were performed using PRIMER (Clarke & Warwick 2001).

Bio-Env analysis

The Bio-Env analysis was carried out using PRIMER to identify the abiotic variables that best explain the assemblage of biotic variables (chlorophyll *a* and zooplankton community). This analysis is based on the unconstrained choice of resemblance matrix appropriate to the data type and utilizes only the rank values of the among sample resemblances (Clarke et al. 2008).

Regression analysis

Salinity is considered to have a prominent role in structuring various water masses in the BoB, and hence a regression analysis using Microsoft excel 2016 was carried out between salinity and the abundances of the different zooplankton taxa in order to understand their affinity towards particular water masses.

Results

Abiotic variables

The monthly climatological data of the SSS in the BoB exhibited heterogeneity in the spatial and temporal distribution (Fig. 1b). Irrespective of the months, the northern basin was less saline

compared to the saltier southern part, and the variance in the SSS was most prominent during August to October (Fig. 1c).

The SSS gradient was used to identify the existence of the salinity fronts and a threshold gradient 0.01 psu / km was considered for the frontal detection. Two frontal zones were identified in the northern part of the BoB, formed as an interface of high and low salinity waters (Fig. 2b). Stations 1, 2, 10 and 11 were observed inside the 1st frontal zone, whereas stations 7, 15 and 16 were in the 2nd frontal zone (Fig. 2b). The SSS gradient across the front varied between 0.01 and 0.033 psu / km. The cross-frontal difference in SSS was found to range between 1 to 3.6 psu (Fig. 2b). In general, the SSS exhibited a pronounced spatial variation, and it ranged between 29.2 and 34.4 psu with lower values in the northern bay compared to the southern part (Fig. 2c). The *in situ* SSS exhibited a significant positive correlation with that of the climatological data of the North Indian Ocean Atlas ($P < 0.001$). Except for the slight spatial displacement in their position with the years, the SSS data acquired through Aquarius for 2012-2014 confirmed the existence of frontal structures in the BoB during the months of September and October (Supplementary Fig. 1). In the BoB, during September-October, the high freshwater discharges from the major rivers results in a prominent low saline region in the northern bay, followed by an intermediate saline frontal zone and a saltier region towards south (Supplementary Fig. 1). The variation among the SSS values of September-October during 2012-2014, and also the *in situ* data of this study, did not show any significant variation (parametric one-way ANOVA, $F_{3,243} = 2.053$, $P = 0.091$). The sea surface density exhibited a pronounced spatial variation, and it ranged between 17.8 and 21.6 kg m⁻³ and was low in most of the sampling locations in the northern bay compared to the southern part (Fig. 2c). The sampling locations in the frontal regions identified through the salinity distribution had an intermediate density between the distinct high and low-density environments, thus delineating the role of salinity in governing the density gradient across the front. The cross-frontal difference in sea surface density varied between 0.8 and 2.8 kg m⁻³. The *in situ* sea surface temperature (SST) did not exhibit prominent spatial variation (28.4 – 29.8°C). Unlike the SSS distribution, the gradient in the SST was quite low ($< 0.01^{\circ}\text{C km}^{-1}$) and the cross-frontal difference was only 0.02 to 0.3°C (Fig. 2d).

The vertical profile of the salinity and potential density exhibited a gradual increase with depth along all transects (Fig. 3a,b). However, the variation was more prominent in the north than the southern transects. In both the frontal zones, an inclined interface region of the distinct salinity characteristics was evident in the upper 50 m (Fig. 3a). In contrast to the salinity and density distribution, the vertical profile of temperature exhibited a gradual decrease with depth (Fig. 3c).

The monthly climatological data of direct precipitation in the BoB in 2001 – 2010 exhibited a pronounced spatio-temporal variation, and experienced the higher rainfall ($>200 \text{ mm month}^{-1}$) from May to October influenced by the southwest monsoon (Fig. 4a). The result of the Pearson correlation analysis of the monthly climatological data (precipitation and SSS) although, exhibited a negative relation; the correlation coefficient was very low ($r = 0.06$) and statistically insignificant ($P = 0.852$).

Similarly, the monthly climatological data of the river discharges into BoB exhibited a prominent temporal variation with higher values ($>40000 \text{ m}^3 \text{ sec}^{-1}$) from July to October (Fig. 4b). The result of the Pearson correlation analysis performed to identify the interrelation of SSS with river discharge exhibited a negative relation and the correlation coefficient although statistically insignificant ($P = 0.398$), was evidently higher ($r = 0.27$) than that observed with precipitation and salinity.

The pH of surface waters varied between 8.15 and 8.38, and with an averaged 8.33 ± 0.05 . In general, the pH gradually decreased with depth along all the latitudinal transects. However, along 19° , 17° and 15° N , the up-sloping of the isolines of pH were observed along the frontal locations (Fig. 5a). The surface DO ranged between 3.8 and 4.9 ml l^{-1} with an average of $4.4 \pm 0.2 \text{ ml l}^{-1}$. Along the frontal ($4.4 \pm 0.3 \text{ ml l}^{-1}$) and non-frontal regions ($4.4 \pm 0.1 \text{ ml l}^{-1}$), the surface DO were mostly the same. Although the spatial variation in the surface DO was not much evident, a sharp gradient was observed in the vertical profiles which were more prominent towards the north (Fig. 5b). Similar to the pH distribution, an uplifting of the isolines of DO was observed along the frontal zones of 15° , 17° and 19° N (Fig. 5b).

The mixed layer depth (MLD) varied from 7 m and 47 m. A clear variation in the MLD was observed between the locations in the frontal and the non-frontal regions (Supplementary Fig. 2a). The average MLD was relatively lower in the frontal zones ($13 \pm 8 \text{ m}$) than the non-frontal regions ($22 \pm 12 \text{ m}$). In the case of the bottom of the thermocline (BT), the depth varied between 133 and 188 m (Supplementary Fig. 2b). Similar to the MLD, the depth of the BT was also relatively less in the frontal zones ($161 \pm 19 \text{ m}$) compared to the non-frontal regions ($167 \pm 16 \text{ m}$).

Nutrients

In general, the nitrate, phosphate and silicate values of the surface waters were relatively lower than in the deeper waters (Fig. 6). The surface nitrate ranged between 0.4 and $3.68 \text{ } \mu\text{M}$, with an average of $2.01 \pm 0.88 \text{ } \mu\text{M}$, whereas phosphate varied between 0.05 and $0.92 \text{ } \mu\text{M}$ (avg. $0.5 \pm 0.22 \text{ } \mu\text{M}$). The surface silicate value ranged between 2.42 and $10.71 \text{ } \mu\text{M}$, with an average of $5.7 \pm 2.04 \text{ } \mu\text{M}$ (Fig.

6c). Inclined isoline of nutrients (nitrate, phosphate, and silicate) were observed along the sampling locations at the frontal zones, i.e., along 19° N (st 1, 2), 17° N (st 7, 10, 11) and 15° N (st 15 and 16).

Biotic components

Chlorophyll a

The *in situ* surface chlorophyll *a* was observed to vary between 0.07 and 0.51 mg m⁻³ during the study with a maximum concentration at station 2 located in the frontal zone at 19° N (Fig. 7c). Most of the locations in the frontal zones exhibited relatively high surface chlorophyll *a* (n = 7, avg. 0.3 ± 0.1 mg m⁻³) compared to the non-frontal locations (n = 24, avg. 0.2 ± 0.1 mg m⁻³) (Fig. 7a). The variation in surface chlorophyll *a* concentration between the frontal and non-frontal regions were found to be statistically significant (Mann-Whitney test: P = 0.025). In the case of the satellite observation, the surface chlorophyll *a* were relatively high in the frontal zones along 15°, 17° and 19°N latitude, and quite low in the non-frontal regions at the 11° and 13°N latitudes (Supplementary Fig. 3). Considering the vertical profile of chlorophyll *a*, the concentration was relatively higher in the upper 50 m compared to the deeper waters in both the frontal and non-frontal locations with a maximum at 10 m depth (Fig. 7a). Although the average chlorophyll *a* concentration in each depth along the frontal locations was higher than that in the non-frontal regions, the disparity in pigment concentration between these two regions was more prominent in the upper water column (up to 20 m) than the deeper water (>20 m - 120 m). The integrated column chlorophyll *a* (75 m) was observed to vary between 4.4 and 28.9 mg m⁻² with a maximum value in the frontal location at station 2 (Fig. 8d). The average column chlorophyll *a* concentration in the frontal location (n = 7, avg. 17.9 ± 6.7 mg m⁻²) was higher than that observed in the non-frontal location (n = 24, avg. 13.9 ± 6.8 mg m⁻²). However, the variation was statistically insignificant (Mann-Whitney test: P = 0.163).

Primary production

The primary production (PP) was determined only at one coastal, and one offshore station along each transect. The surface production was found to vary between 0.07 and 10.25 mg C m⁻³ day⁻¹ with an average of 3.06 ± 2.94 mg C m⁻³ day⁻¹ (Fig. 7e). Among the sampling locations in the frontal zones, the PP was monitored at two locations and the value was observed to be remarkably higher (n = 2, avg. 7.14 ± 4.4 mg C m⁻³ day⁻¹) compared to the non-frontal region (n = 8, avg. 2 ± 1.5 mg C m⁻³ day⁻¹). The vertical profile of PP exhibited a sharp decline below 10 m and the average PP was observed to be highest at the surface in frontal locations and at the 10 m in the non-frontal locations (Fig. 7b). Although the PP at each depth was higher in the frontal locations compared to non-frontal regions, the variation between them was more prominent in the upper 10 m (Fig. 7b). The integrated

column PP (0-75 m) varied between 19 and 211 mg C m⁻² day⁻¹ during the study period (Fig. 7f). The column PP in the frontal locations (n = 2, avg. 195 ± 23 mg C m⁻² day⁻¹) was characterized by higher values (1.7 times) compared to the non-frontal locations (n = 8, avg. 114 ± 83 mg C m⁻² day⁻¹).

Specific growth rate

The specific growth rate of the phytoplankton was measured in the station locations (total 10), where, both primary production and chlorophyll *a* were estimated, and it varied between 0.5 and 30.1 (Supplementary Fig. 4). It was relatively higher in the frontal locations (n = 2, avg. 20.7 ± 13.4 mg C Chl *a*⁻¹ m⁻³ day⁻¹) compared to the non-frontal locations (n = 8, avg. 9.1 ± 5.8 mg C Chl *a*⁻¹ m⁻³ day⁻¹).

Mesozooplankton biomass and abundance

The integrated mesozooplankton biomass of the upper two layers (mixed layer depth and thermocline) varied between 0.03 and 0.53 ml m⁻³ with an average of 0.18 ± 0.11 ml m⁻³ (n = 31, Fig. 7g). The biomass was evidently higher in the frontal zones (n = 7, avg. 0.3 ± 0.12 ml m⁻³) compared to the non-frontal regions (n = 24, avg. 0.1 ± 0.1 ml m⁻³). The variation in the biomass between the fronts and the non-frontal locations was significant (Mann-Whitney test: P = 0.002). In the case of the abundance, the minimum value was observed at station 27 (50 ind m⁻³) in the non-frontal region, whereas abundance was maximum at station 16 (1143 ind m⁻³) in the frontal zone (Fig. 7h). In general, the abundance was higher in the frontal zones (n = 7, avg. 506 ± 305 ind m⁻³) compared to the non-frontal regions (n = 24, avg. 244 ± 171 ind m⁻³) and this variation was statistically significant (Mann-Whitney test: P = 0.011).

Mesozooplankton composition

A total of 24 zooplankton taxa were observed among which Copepoda dominated in all the sampling locations contributing 58 to 97 % of the total zooplankton population (Table 2). Chaetognatha, ostracoda, euphausiid and copelata were the other abundant taxa sharing >1% of the total zooplankton population. In the frontal zone, of the total 22 groups of zooplankton taxa observed, copepoda contributed 92.5% of the total population (Table 2). Among the non-copepoda taxa, chaetognatha formed the only group sharing >1% of the total population. In the non-frontal regions, a total of 24 zooplankton taxa were observed. Although copepoda also dominated in the non-frontal region, their contribution to the total population (86.8%) was comparatively lower than in the frontal zone. The other abundant zooplankton taxa (>1%) in the non-frontal regions were chaetognatha, ostracoda, euphausiida and copelata. In the frontal zones, the abundance of copepods (n= 7, avg. 468 ± 318 ind m⁻³) was 2.2 times higher than that observed in the non-frontal regions (n = 24, avg. 212 ±

147 ind m⁻³) and the variation was statistically significant (P = 0.005) (Table 2). Except ostracoda, foraminifera, gastropoda larvae, and stomatopoda, all the other zooplankton taxa which were observed in both the regions exhibited relatively higher abundance in the frontal zones compared to the non-frontal regions (Table 2).

Diurnal variability

It was observed that in the diurnal locations of both the frontal zones (st 1 and st 7 in the 1st and the 2nd frontal zones respectively), the biomass was relatively higher during the day compared to night, whereas in the non-frontal locations (8 stations) it was higher during the night (Fig. 8). Zooplankton abundance had a similar pattern of distribution in the frontal and non-frontal regions (Fig. 8). Among the zooplankton taxa, copepoda, siphonophora, ostracoda, amphipoda and pteropoda exhibited higher day abundance in the frontal region, whereas, in the non-frontal region, they exhibited an opposite trend in their distribution (Fig. 8). Chaetognatha, copelata, salpa, and doliolida had a higher abundance at night in both the frontal and non-frontal regions, with a relatively higher night / day ratio in the frontal region (Fig. 8).

Data analyses

Sampling locations of the front and non-frontal regions exhibited a difference in their position along the axis of CAP based on the abundance of zooplankton taxa (Fig. 9). The squared canonical correlations of the axis (δ^2) was 0.57. The variability observed in the zooplankton community structure during the study was further investigated using the MVDISP algorithm. The variability was higher in the sampling locations of the non-frontal region (Dispersion factor value = 1.024), compared to the locations of the frontal zone (Dispersion factor value = 0.678). However, the Indices of Multivariate Dispersion (IMDs) exhibited a negative value (-0.347) in the pairwise comparisons among frontal, and non-frontal locations, indicating that, in the case of the zooplankton community structure, similarities in station locations within each group (frontal, and non-frontal) were greater than the similarities present between these 2 groups. In the one-way ANOSIM analysis, it was found that the zooplankton community in the frontal zone is significantly distinguishable from the community in the non-frontal region (Global R = 0.178, p = 0.047).

A quadratic regression analysis was performed to assess the preferred water mass of the various zooplankton taxa. The resultant binomial curvilinear regression line was dome shaped for most of the zooplankton taxa (Fig. 10).

The result of the Bio-Env analysis indicated that the combination of nitrate, DO and potential density were the most important factors that best explained the variability in the abundance and distribution of the biotic variables (Table 3).

Discussion

The hydrodynamics associated with mesoscale physical processes provides the auxiliary energy for augmenting the primary production, leading to rich resources for the superior growth conditions of the apex trophic levels in the pelagic food web (Bakun 2006). Marine fronts, a region where auxiliary energy generated by hydrodynamic convergences concentrates in disproportionate quantities in small areas gain significance in the ecological process studies in the global ocean (Acha et al. 2015). Two river plume fronts identified through the SSS gradient were observed in the northern BoB (Fig. 2). These frontal zones were found at the interface of two distinct salinity water masses with sharp horizontal gradient (0.01 and 0.033 psu / km). Considering the six types of fronts of large marine ecosystems, the inclusion of BoB as a river plume front is significant (Tables 1 and 5 in Belkin et al. 2009). The cross-frontal difference of 1 to 3.6 psu in SSS was in accordance with the earlier record in the northern BoB (Shetye et al. 1991). Although the cross-frontal difference in SSS can be as large as 2–3 psu, the typical difference in the large frontal system is usually observed to be between 0.3–1.0 psu (Belkin et al. 2009) and thus the evident cross-frontal difference in the BoB clearly delineates their status as a salinity front. The sea surface density, displaying sharp gradients in the frontal zones in agreement with the SSS, indicated the role of salinity in the frontogenesis in the BoB.

The vertical profile of the salinity and water density in the upper 50 m manifested the frontal zone as a region separating water masses of different hydrographic characteristics. The vertical profile of pH and DO also affirmed the existence of the narrow three-dimensional frontal zones in the study region (Fig. 6). However, the less variation in SST (28.4 – 29.8°C) and low SST gradient ($< 0.01^{\circ}\text{C km}^{-1}$) in comparison to the SST gradient observed in the frontal region of Arabian Sea (0.04 – 0.08°C km⁻¹) (Vipin et al. 2015), the western counterpart of BoB, point towards the weak influence of temperature in the frontogenetic process.

The enormous freshwater input from the major perennial rivers (Ganges, Brahmaputra, Irrawaddy and Mahanadi) contributing ~75 % of the total river runoff to the head of the BoB (Frontal zone 1) and the river Godavari to the central BoB (Frontal zone 2) contributed to the dilution of the salinity of the bay resulting in sharp horizontal gradient in salinity (Chaitanya et al. 2014). The plume of the low saline coastal waters extending offshore led to isopycnal mixing with

the high saline offshore water across the boundary of the interface and resulted into distinct frontal zones in the northern BoB. The influence of freshwater plume in the frontogenetic processes, along the tropical Atlantic and Pacific Ocean by major rivers like Mississippi, Amazon and Yangtze (Tian et al. 1993, Lentz & Limeburber 1995, Lohrenz et al. 1999), substantiates observations about the role of salinity in the genesis of oceanic fronts. The negative interrelation between the monthly climatological data of river discharge and SSS is expected because of the prominent influence of freshwater in lowering salinity. However, the insignificant correlation coefficient between river discharge and SSS might be because of the lag in the river influx and corresponding decrease in the salinity (Fig. 4).

Both river discharge and precipitation have been found to have a role in the salinity distribution of the BoB (Akhil et al. 2014, Chaitanya et al. 2015), but the expected negative interrelation between the SSS and precipitation was not very strong ($r = -0.06$, $P = 0.852$). The lag between the peak in precipitation and the consequent drop in SSS can be attributed to this weak negative relation. The disparity between the influence of river discharge and the direct precipitation in the frontogenesis of the BoB happens because the locations of river discharges does not change temporally, and, the continuous fresh water influx during the monsoon contributes to the maintenance of the frontal structure. On the contrary, the influence of precipitation on the spatial variation of salinity depends on the duration and spatial cover of precipitation with changes happening only for a short period producing only a local effect on the lowering of SSS. Hence, compared to the river influxes the direct precipitation was less significant in the frontogenesis of BoB.

Although the river plume fronts were evident in the BoB during September and October, it was a prerequisite to identify how the scenario resembles with the general pattern of the freshwater plume and salinity distribution in this region. The significant positive correlation ($P < 0.001$) between the *in situ* and the monthly atlas data validates the present SSS as a representative of salinity distribution for this period in the BoB. The insignificant variation in the SSS retrieved from Aquarius (2012 to 2014) and the present data ($P = 0.091$) also helped to decipher this concern. The existence of the low-saline water in the vicinity of the major rivers in the northern part, and the small patch of the low-saline tongue along the Indian coast between 15° to 19° , and the intermediate saline water with a higher gradient in SSS during 2012 to 2014, indicated the general nature of the river plume fronts in the BoB. However, there was small temporal variability in the spatial structure of the SSS (Supplementary Fig. 1). Of the multiple factors governing the spatial distribution of SSS from the vicinity of the river mouth to the offshore region, the influence of coastal currents, wind patterns and the amount of river discharges are the primary ones (Lentz & Limeburber 1995, Grimes & Kingsford

1996). In the western BoB, the East India Coastal Current (EICC) flows northward from February to September with a strong peak in March – April. Interior Ekman pumping, remote alongshore wind and equatorial forcing all contribute to the March - April peak, whereas the local alongshore wind forms the only primary driving force in the remaining course of the northward flow (McCreary et al. 1996). The southward flow of the EICC during October to January is mostly governed by the local alongshore wind and interior Ekman pumping. The propagation of freshwater plume along the western BoB has been found to be consistent with alongshore advection of EICC (Chaitanya et al. 2014). Hence, depending on the strength of the local and remote alongshore winds and Ekman pumping, the dynamics of EICC influence the spatial distribution of the freshwater plume as evidenced in the Aquarius dataset. The annual variability in the freshwater discharge from the major rivers is also evident in the BoB (Gates et al. 2000). All of these factors contribute to the spatial variation in the salinity resulting in the spatial displacement of the intermediate saline frontal zones documenting. The climatological monthly SSS of the BoB helped to understand the persistence of the frontal structures along a temporal scale. Although the north-south gradient in SSS was observed every month, the variance was more prominent during August – October (Fig. 1) when the freshwater influx from the major rivers is high (Jian et al. 2009). Hence, it can be postulated that, although the frontogenesis can happen at a smaller scale throughout the year, it becomes much obvious during August-October when the freshwater discharges are high.

Fronts are designated as vertically inclined interfaces between water masses of distinct hydrographic properties where the intense mixing of nutrient-rich subsurface waters forms a conducive environment supporting high biotic production (Lohrenz et al. 1999). The presence of inclined interfaces in the vertical profiles of nutrients (nitrate, phosphate, and silicate) in the frontal zones (Fig. 6) confirms that fronts are important zones of nutrient pumping and replenishment in the surface waters (Franks & Chen 1996). Hence, a comprehensive understanding of the implications of this dynamic frontal system on the biotic community gains relevance (Corredor et al. 2003, Powell & Ohman 2015).

The observed high chlorophyll *a* and enhanced primary production (both surface and column) in the frontal zones compared to the non-frontal locations validate frontal region as a conducive region promoting higher growth and proliferation of the phytoplankton community in the BoB. Earlier observation of higher chlorophyll *a* in the Mississippi river plume front by Lohrenz et al. (1999) also supports the productive nature of the frontal region. The nutrient replenishment of surface waters occurring in concurrence with the isopycnal mixing during the frontogenesis favored the higher primary production. The mixing between two adjacent water masses of discrete hydrographic

properties provide the optimum conditions (nutrients, warmth) for the increased preponderances of the phytoplankton community that neither water masses might contain alone (Quartly & Srokosz 2003). Hence, fronts are best defined as “typically the site of enhanced phytoplankton biomass” (Franks 1992a). However, riverine nutrients may play a linear relationship to biotic productivity from coast to offshore (Singh & Ramesh 2011). Hence it was important to separate the role of fronts from the direct influence of nutrients of the riverine inputs. We observed the higher productivity in the intermediate saline frontal zones than the low saline and high saline regions. This productivity pattern evidently supports the influence of fronts on the phytoplankton community.

Zooplankton biomass and abundance were also evidently higher in the frontal zones and the significant variation in biomass ($P = 0.002$) and abundance ($P = 0.011$) among two groups (front, and non-front) clearly indicates the positive influence of fronts on the zooplankton biomass and abundance. This is in contrast to the observation of Jasmine et al. (2009) where the microbial loop regulated zooplankton abundance, and showed less variation among frontal and other locations during austral summer in the southern ocean region. The discrete existence of the frontal locations in the CAP plots (based on zooplankton abundance) affirms the distinctness of the frontal regions in the BoB. The higher zooplankton abundance in the frontal zones could be the outcome of either new recruits of organisms, a consequence of differential growth and mortality, or aggregation due to physical forces. Although the zooplankton mortality or growth rate was not estimated, the food availability in terms of higher phytoplankton biomass in the frontal regions might have supported the zooplankton community aggregated by hydrodynamic convergences. The relatively high zooplankton abundance (2.1 times) compared to that of phytoplankton biomass (1.5 times) in the frontal regions substantiates the influence of food availability on the congregated zooplankton. The higher biomass and abundance of the zooplankton community in the Mississippi river plume front in the Atlantic Ocean (Grimes & Finucane 1991) further validates the positive influence of fronts on the zooplankton community. The higher abundance of zooplankton in the frontal region helped to elucidate the vertical profile of chlorophyll *a* and PP. The surface zooplankton (epiplankton) has been observed to display the subsurface maxima in their vertical distribution (Longhurst 1976, Rezai et al. 2011). This subsurface inhabitation and subsequent utilization of the phytoplankton resulted in the less variation in the chlorophyll *a* and PP in the subsurface water column compared to surface waters (0 – 10 m). Hence, it can be anticipated that frontal zones play a crucial role in the energy transfer in the BoB.

Copepoda exhibited a markedly higher abundance and an increased percentage of contribution to the total zooplankton population in the frontal zone (Table 2). Copepoda, because of their unique

proficiency to remotely detect prey through hydromechanical and chemical cues along with their feeding-current feeding, might have out-competed the other zooplankton taxa in the utilization of the food-rich environment of the frontal regions (Mauchline 1998, Kiørboe 2011). Further, their smaller size, diverse feeding guilds and the low generation time makes them the most suitable to efficiently utilizing resources of productive areas, like frontal zones or cold core eddy regions (Lopes et al. 2016). Moreover, the dome-shaped curvilinear binomial regression line obtained based on the interrelation of their abundance with salinity indicates their affinity towards the intermediate saline frontal water mass. Although there can be species specific variation in the food preferences and tolerance towards the physical environment, the result indicates the overall positive influence of fronts on the copepod community. Chaetognatha, a major carnivorous zooplankton taxa in both the eastern and western part of the northern Indian Ocean (Kusum et al. 2011, 2014 a,b, Nair et al. 2015), formed the second abundant taxon in the frontal zones. The vital role of copepod as a major prey contributing to the higher abundance of chaetognatha population has been recorded from various parts of the global ocean (Stuart & Verheye 1991, Kehayias & Ntakou 2008). Hence, the increased abundance of copepods (2.3 times) in the frontal regions might have helped in the sustenance of the higher abundance of chaetognatha (2 times).

Besides chaetognatha, the higher abundance of the most of the other predominant taxa (decapod larvae, euphausiida) points towards their aggregation in the food-rich environment of the frontal zones compared to the non-frontal locations. The dome shaped curvilinear binomial regression line observed in most of the zooplankton taxa clearly supports their aggregation in the intermediate saline frontal water mass. Reports on physical aggregation of zooplankton by surface currents contributing to the higher abundance in many frontal regions affirm our observation (Franks 1992b, Hetland et al. 2002). However, taxa like foraminifera, gastropoda, and stomatopoda had lower abundance in the frontal zone (Table 2). The food-rich environment of the frontal region might be favorable for a majority of zooplankton taxa, but, the physiological challenges imposed by thermal or haline stresses characteristic of these regions might limit the abundance of some organisms (Olson 2002).

The diurnal distribution of the zooplankton community exhibited a contrasting trend in the frontal and the non-frontal locations. Mesozooplankton abundance is reported to be higher in surface waters at night in concurrence to the diel vertical migration (Lampert 1989, Doney & Steinberg 2013) which was also evident in the present study. However, it was higher during the day in the frontal zone. In aquatic ecosystems, changes in the vertical distribution along diel scales provide zooplankton with many ecological benefits, among which the metabolic advantages of feeding in warm food-rich surface waters at night and the protection from light dependent mortality imposed by

visually oriented predators, are considered the most beneficial (Lampert 1989). The contrasting trend observed in the frontal regions can be the result of the strategy of optimum exploitation of food resources by the zooplankton community. In the barren tropical oceans, frontal regions often are a 'natural oasis' with a bountiful supply of food resources for the zooplankton community. The food rich environment in surface waters of the frontal regions might have refrained the zooplankton community from migrating down to deeper waters where food resources are comparatively poor. Moreover, the relatively higher night / day ratio of the abundance of the chaetognatha in the frontal regions also reinforced the higher day abundance of the zooplankton community in the frontal zones. Being a voracious carnivore, chaetognatha are known to impose a significant effect on the abundance and distribution of the zooplankton community (Froneman & Pakhomov 1998, Pakhomov et al. 1999). Their higher night abundance and increased predatory activity on the zooplankton community might have resulted in the observed disparity in the diel distribution pattern in the frontal zones.

The result of the MVDISP algorithm demonstrated the variability in the zooplankton community structure of the frontal zones and other locations. The higher homogeneity in the zooplankton community structure in the fronts resulted in the lower dispersion value compared to the other locations. Frontal zones are often considered as productive regions characterized by sharp gradients in the environmental variables (Sournia 1994, Belkin et al. 2009). Thus, the abundance of the zooplankton taxa, which were physiologically adapted to the dynamic environment of fronts and also efficient in harvesting the food resources of this productive region, contributed to the less variability in the zooplankton community structure. This, in turn, resulted in the greater dissimilarities among the community structure of the frontal and non-frontal regions than the similarities they share (as indicated by the negative IMD value).

The dissimilar characteristics of the zooplankton community evidenced through the MVDISP algorithm in frontal zones and other sampling locations were further reflected in the one-way ANOSIM analysis. The significantly distinguishable community between the frontal and the non-frontal zones (Global $R = 0.178$, $p = 0.047$) might be the result of the variation in the auxiliary energy required for the enhanced biotic production.

The potential density, nitrate and DO (through BIOENV analysis) were identified as the most prominent factors that best explained the variability occurring in the abundance and distribution of the phytoplankton and zooplankton community. As fronts are mostly generated as an interface of different potential density water masses (Franks 1992a, Bakun 2006) where the intense mixing and enrichment of nutrients aid in supporting higher plankton production (Lohrenz et al. 1999), the

combination of these factors identified through BIOENV, governing the higher production in the frontal zones of BoB is validated.

The higher abundance of fish larvae in the frontal zone compared to other regions might have happened by the spatial displacement resulting from the hydrodynamic convergence in the frontal zone (Grimes & Finucane 1991). In addition, fish larvae are known to aggregate in productive oceanic regions characterized by higher prey density (Alemany et al. 2014). The higher food availability in terms of both phytoplankton and zooplankton (copepoda) also contributed to their higher abundance in the frontal zone. Copepoda are often considered as preferred prey and the prime constituent of the diet of many pelagic fishes and fish larvae (Heath & Lough 2007, Pepin & Penney 2000). Hence, the higher abundance of copepod, contributing about 92.5% of the total zooplankton population in the frontal zones played a significant role towards making this region as a better breeding and nursing ground leading to the increased larval abundance. Fishes often prefer to spawn in regions where better feeding opportunities help in the enhanced growth and survival rates of their highly vulnerable early life stages (Swalethorp et al. 2015). Studies related to the aggregation of fish larvae in the tropical river plume frontal zones compared to its contiguous water masses in response to their preferred prey availability are well-addressed (Grimes & Finucane 1991, Govoni 1993). The incident increased abundance of the higher trophic levels (herbivorous, carnivorous zooplankton and fish larvae) in the frontal region in this study points it as a zone persisting for a considerable period and allowing for the efficient energy transfer to the successive trophic levels (Olson & Backus 1985).

Acknowledgements:

Our sincere gratitude to Dr. Igor Belkin, University of Rhode Island, for his detail suggestions to formulate the MS. We thank the Director, National Institute of Oceanography, and the Director, CMLRE, Kochi, for providing the facilities. This study was carried out under the program Marine Research on Living Resources (MR-LR) funded by the Ministry of Earth Sciences, Govt. of India. This is NIO contribution ****.

Literature Cited

- Acha EM, Piola A, Iribarne O, Mianzan H (2015) Ecological Processes at Marine Fronts: Oases in the Ocean. Springer.
- Akhil VP, Durand F, Lengaigne M, Vialard J, Keerthi MG, Gopalakrishna VV, Deltel C, Papa F, de Boyer Montégut C (2014) A modeling study of the processes of surface salinity seasonal cycle in the Bay of Bengal. *J Geophys Res Oceans* 119: 3926–3947.

- Albaina A, Irigoien X (2004) Relationships between frontal structures and zooplankton communities along a cross-shelf transect in the Bay of Biscay (1995 to 2003). *Mar Ecology Progress Series*, 284, 65-75.
- Alemaný D, Acha EM, Iribarne O (2014) Marine fronts are important fishing areas for demersal species at the Argentine Sea (Southwest Atlantic Ocean). *J Sea Res* 87: 56-67.
- Anderson MJ, Willis TJ (2003) Canonical analysis of principal coordinates: a useful method of constrained ordination for ecology. *Ecology* 84: 511-525.
- Antonov JI, Seidov D, Boyer TP, Locarnin RA, Mishonov AV, Garcia HE (2010) World Ocean Atlas 2009, 2: Salinity. NOAA Atlas NESDIS 69, NOAA, U.S. Government Printing Office, Washington D.C.
- Bakun A (2006) Fronts and eddies as key structures in the habitat of marine fish larvae: opportunity, adaptive response and competitive advantage. *Sci Mar* 70S2: 105-122.
- Belkin IM, Cornillon P (2003) SST fronts of the Pacific coastal and marginal seas. *Pac Oceanogr* 1: 90-113.
- Belkin IM, Cornillon PC, Sherman K (2009) Fronts in large marine ecosystems. *Prog Oceanogr* 81: 223-236.
- Chaitanya AVS, Lengaigne M, Vialard J, Gopalakrishna VV, Durand F, Kranthikumar C, Amritash S, Suneel V, Papa F, Ravichandran M (2014) Salinity measurements collected by fishermen reveal a “river in the sea” flowing along the eastern coast of India. *B Am Meteorol Soc* 95: 1897-1908.
- Chaitanya AVS, Durand F, Mathew S, Gopalakrishna VV, Papa F, Lengaigne M, Vialard J, Kranthikumar C, Venkatesan R (2015) Observed year-to-year sea surface salinity variability in the Bay of Bengal during the 2009–2014 period. *Ocean Dynamics* 65: 173-186.
- Chatterjee A, Shankar D, Shenoi SSC, Reddy GV, Michael GS, Ravichandra, M, Gopalakrishna VV, RamaRao EP, Udayabhaskar TVS, Sanjeevan VN (2012) A new atlas of temperature and salinity for the North Indian Ocean. *J Earth Syst Sci* 121: 559–593.
- Clarke KR, Warwick RM (2001) *Change in Marine Communities: An Approach to Statistical Analysis and Interpretation*. 2nd edition, Plymouth, UK.
- Clarke KR, Somerfield PJ, Gorley RN (2008) Testing of null hypotheses in exploratory community analyses: similarity profiles and biota-environment linkage. *J Exp Mar Biol Ecol* 366: 56-69.
- Clifford HT, Stephensen W (1975) *An Introduction to Numerical Classification*. Academic Press, New York.
- Corredor J, Morell J, López J, Armstrong R, Dieppa A, Cabanillas C, Cabrera A, Hensley V (2003) Remote continental forcing of phytoplankton biogeochemistry: observations across the “Caribbean-Atlantic front”. *Geophys Res Lett* doi:10.1029/2003GL018193.
- Doney SC, Steinberg DK (2013) Marine biogeochemistry: the ups and downs of ocean oxygen. *Nature Geosci* 6: 515-516.

- Dyson N, Jitts HR, Scott BD (1965) Techniques for measuring oceanic primary production using radioactive carbon. CSIRO Tech Paper 18: 1-12.
- Evans RH, Brown OB (1981) Propagation of thermal fronts in the Somali Current system. *Deep Sea Res I* 28: 521-527.
- Fernandes V (2008) The effect of semi-permanent eddies on the distribution of mesozooplankton in the central Bay of Bengal. *J Mar Res* 4: 465–488.
- Fernandes V, Ramaiah N (2013) Mesozooplankton community structure in the upper 1,000 m along the western Bay of Bengal during the 2002 fall intermonsoon. *Zool Stud* 52: 1-16.
- Franks PJS (1992a) Phytoplankton blooms at fronts: patterns, scales, and physical forcing mechanisms. *Rev Aquat Sci* 6: 121-137.
- Franks PJS (1992b) Sink or Swim: accumulation of biomass at fronts. *Mar Ecol Prog Ser* 82: 1-12.
- Franks PJ, Chen C (1996) Plankton production in tidal fronts: a model of Georges Bank in summer. *J Mar Res* 54: 631-651.
- Froneman PW, Pakhomo EA (1998) Trophic importance of the chaetognaths *Eukrohnia hamata* and *Sagitta gazellae* in the pelagic system of the Prince Edward Islands (Southern Ocean). *Polar Biol* 19: 242-249.
- Gates LD, Hagemann S, Golz C (2000) Observed historical discharge data from major rivers for climate model validation. MPI-Report, 307: Max-Planck-Institut für Meteorologie, Hamburg.
- Gomes HR, Goes JI, Saino T (2000) Influence of physical processes and freshwater discharge on the seasonality of phytoplankton regime in the Bay of Bengal. *Cont Shelf Res* 20: 313-330.
- Govoni JJ (1993) Flux of larval fishes across frontal boundaries: examples from the Mississippi River plume front and the western Gulf Stream front in winter. *B Mar Sci* 53: 538-566.
- Grasshoff K (1983) Determination of oxygen. In: Grasshoff K, Ehrhardt M, Kremling K (Eds.), *Methods of Sea Water Analysis*, Verlag Chemie, Weinheim, pp. 61–72.
- Grimes CB, Finucane JH (1991) Spatial distribution and abundance of larval and juvenile fish, chlorophyll and macrozooplankton around the Mississippi River discharge plume, and the role of the plume in fish recruitment. *Mar Ecol Prog Ser* 75: 109-119.
- Grimes CB, Kingsford MJ (1996) How do riverine plumes of different sizes influence fish larvae: do they enhance recruitment? *Mar Freshwater Res* 47: 191-208.
- Harris R, Wiebe P, Lenz J, Skjoldal HR, Huntley ME (Eds) (2000) *ICES Zooplankton Methodology Manual*. Academic Press, London.
- Heath MR, Lough RG (2007) A synthesis of large-scale patterns in the planktonic prey of larval and juvenile cod (*Gadus morhua*). *Fisheries Oceanogr* 16: 169-185.
- Hetland RD, McGillicuddy DJ, Signell RP (2002) Cross-frontal entrainment of plankton into a buoyant plume: the frog tongue mechanism. *J Mar Res* 60: 763-777.

- Ismail M (2011) Observation on barrier layer and role of positive water balance on inversion layer dynamics in the Bay of Bengal. MSc Thesis, Cochin University of Science and Technology, Cochin.
- Jasmine P, Muraleedharan KR, Madhu NV et al 2009. Hydrographic and productivity characteristics along 45°E longitude in the southwestern Indian Ocean and Southern Ocean during austral summer 2004. *Mar Ecol Prog Ser* 389: 97-116.
- Jian J, Webster PJ, Hoyos CD (2009) Large-scale controls on Ganges and Brahmaputra river discharge on intraseasonal and seasonal time-scales. *QJR Meteorol Soc* 135: 353-370.
- Kehayias G, Ntakou E (2008) Abundance, vertical distribution and feeding of chaetognaths in the upper 50 m layer of the eastern Aegean Sea. *J Nat Hist* 42: 633-648.
- Kjørboe T (2011) What makes pelagic copepods so successful? *J Plankton Res* 33: 677-685.
- Kusum KK, Vineetha G, Raveendran TV, Muraleedharan KR, Nair M, Achuthankutty CT (2011) Impact of oxygen-depleted water on the vertical distribution of chaetognaths in the northeastern Arabian Sea. *Deep-Sea Res I* 58: 1163-74.
- Kusum KK, Vineetha G, Raveendran TV, Nair VR, Muraleedharan KR, Achuthankutty CT, Joseph T (2014a) Chaetognath community and their responses to varying environmental factors in the northern Indian Ocean. *J Plankton Res* 36: 1146-1152.
- Kusum KK, Vineetha G, Raveendran TV, Muraleedharan KR, Biju A, Achuthankutty CT (2014b) Influence of upwelling on distribution of chaetognath (zooplankton) in the oxygen deficient zone of the eastern Arabian Sea. *Cont Shelf Res* 78: 16-28.
- Lampert W (1989) The adaptive significance of diel vertical migration of zooplankton. *Funct Ecol* 3: 21-27.
- Laubscher RK, Perissinotto R, McQuaid CD (1993) Phytoplankton production and biomass at frontal zones in the Atlantic sector of the Southern Ocean. *Polar Biol* 13: 471-481.
- Lentz SJ, Limeburner R (1995) The Amazon River Plume during AMASSEDS: Spatial characteristics and salinity variability. *J Geophys Res Oceans* 100: 2355-2375.
- Levitus S (1982) Climatological Atlas of the World Oceans. NOAA Professional Paper 13: U.S. Govt. Printing Office, Washington D.C.
- Lohrenz SE, Fahnenstiel GL, Redalje DG, Lang GA, Dagg MJ, Whitledge TE, Dortch Q, 1999. Nutrients, irradiance, and mixing as factors regulating primary production in coastal waters impacted by the Mississippi River plume. *Cont Shelf Res* 19: 1113-1141.
- Longhurst AR (1976) Interactions between zooplankton and phytoplankton profiles in the eastern tropical Pacific Ocean. *Deep Sea Res* 23: 729-754.
- Lopes RM, Marcolin CR, Brandini FP (2016) Influence of oceanic fronts on mesozooplankton abundance and grazing during spring in the south-western Atlantic. *Mar Freshwater Res* 67: 626-635.

- Madhu NV, Maheswaran PA, Jyothibabu R, Sunil V, Revichandran C, Balasubramanian T, Gopalakrishnan TC, Nair KKC (2002) Enhanced biological production off Chennai triggered by October 1999 super cyclone (Orissa). *Curr Sci* 82: 1472-1479.
- Maneesha K, Sarma VVSS, Reddy NPC, Sadhuram Y, Murty TR, Sarma VV, Kumar MD (2011) Meso-scale atmospheric events promote phytoplankton blooms in the coastal Bay of Bengal. *J Earth Sys Sci* 120: 773-782.
- Mauchline J (1998) *The biology of calanoid copepods*. Academic press, London.
- McCreary JP, Han W, Shankar D, Shetye SR (1996) Dynamics of the East India Coastal Current: 2. Numerical solutions. *J Geophys Res* 101: 13993-14010.
- Muraleedharan KR, Jasmine P, Achuthankutty CT, Revichandran C, Dinesh kumar PK, Anand P, Rejomon G (2007) Influence of basin scale and mesoscale physical processes on biological productivity in the Bay of Bengal during the summer monsoon. *Prog Oceanogr* 72: 364-383.
- Nair VR, Kusum KK, Gireesh R, Nair M (2015) The distribution of the chaetognath population and its interaction with environmental characteristics in the Bay of Bengal and the Arabian Sea. *Mar Biol Res* 11: 269-282.
- Olson DB, Backus RH (1985) The concentrating of organisms at fronts: a cold-water fish and a warm-core Gulf Stream ring. *J Mar Res* 43: 113-137.
- Olson DB (2002) Biophysical dynamics of ocean fronts. *Biological–Physical Interactions in the Sea. The Sea*, vol. 12. Wiley, New York, USA.
- Owen RW (1981) Fronts and Eddies in the Sea: Mechanisms, Interactions and Biological Effects. In: Longhurst AR (ed) *Analysis of marine ecosystems*. Academic Press, New York, p 197-233.
- Pakhomov EA, Perissinotto R, Froneman PW (1999) Predation impact of carnivorous macrozooplankton and micronekton in the Atlantic sector of the Southern Ocean. *J Mar Sys* 19: 47-64.
- Papa F, Bala SK, Pandey RK, Durand F, Gopalakrishna VV, Rahman A, Rossow WB (2012) Ganga-Brahmaputra river discharge from Jason-2 radar altimetry: an update to the long-term satellite-derived estimates of continental freshwater forcing flux into the Bay of Bengal. *J Geophys Res Oceans* 117: C11021.
- Pepin P, Penney R (2000) Feeding by a larval fish community: impact on zooplankton. *Mar Ecol Prog Ser* 204: 199-212.
- Powell JR, Ohman MD (2015) Covariability of zooplankton gradients with glider-detected density fronts in the Southern California Current System. *Deep Sea Res II* 112: 79-90.
- Prasanna Kumar S, Muraleedharan PM, Prasad TG, Gauns M, Ramaiah N, De Souza SN, Sardesai S, Madhupratap M (2002) Why is the Bay of Bengal less productive during summer monsoon compared to the Arabian Sea? *Geophys Res Lett* 29(24): doi:10.1029/2002GL016013.
- Prasanna Kumar S, Nuncio M, Narvekar J, Kumar A, Sardesai S, De Souza SN, Gauns M, Ramaiah N, Madhupratap M (2004) Are eddies nature's trigger to enhance biological productivity in the Bay of Bengal?. *Geophys Res Lett* 31: L07309.

- Prasanna Kumar S, Nuncio M, Ramaiah N, Sardesai S, Narvekar J, Fernandes V, Paul JT (2007) Eddy-mediated biological productivity in the Bay of Bengal during fall and spring intermonsoons. *Deep Sea Res I* 54: 1619-1640.
- Qasim SZ (1977) Biological productivity of the Indian Ocean. *Indian J Mar Sci* 6: 122-137.
- Quartly G D, Srokosz MA (2003) A plankton guide to ocean physics: colouring in the currents round South Africa and Madagascar. *Ocean Challenge* 12: 19– 23.
- Rao RR, Girish Kumar MS, Ravichandran M, Samala BK, Sreedevi N (2006a) Observed mini-cold pool off the southern tip of India and its intrusion into the south central Bay of Bengal during summer monsoon season. *Geophys Res Lett* 33: L06607.
- Rao KH, Smitha A, Ali MM (2006b) A study on cyclone induced productivity in south-western Bay of Bengal during November-December 2000 using MODIS (SST and chlorophyll-*a*) and altimeter sea surface height observations. *Indian J Mar Sci* 35: 153-160.
- Rezai H, Yusoff FM, Othman BHR (2011) Vertical distribution of zooplankton and copepod community structure in the Straits of Malacca. *J Persian Gulf* 2: 17-24.
- Sarma VVSS, Delabehra HB, Sudharani P, Remya R, Patil JS, Desai DV (2015) Variations in the inorganic carbon components in the thermal fronts during winter in the northeastern Arabian Sea. *Mar Chem* 169: 16–22.
- Scales KL, Miller PI, Embling CB, Ingram SN, Pirotta E, Votier SC (2014) Mesoscale fronts as foraging habitats: composite front mapping reveals oceanographic drivers of habitat use for a pelagic seabird. *J R Soc Interface* 11:20140679. <http://dx.doi.org/10.1098/rsif.2014.0679>.
- Shetye SR, Shenoi SSC, Gouveia AD, Michael GS, Sundar D, Nampoothiri G (1991) Wind-driven coastal upwelling along the western boundary of the Bay of Bengal during the southwest monsoon. *Cont Shelf Res* 11: 1397-1408.
- Shetye SR, Gouveia AD, Shankar D, Shenoi SSC, Vinayachandran P, Sundar N, Michael GS, Nambodiri G (1996) Hydrography and circulation in the western Bay of Bengal during the northeast monsoon. *J Geophys Res* 101: 14011–14025.
- Singh A, Ramesh R (2011) Contribution of riverine dissolved inorganic nitrogen flux to new production in the coastal northern Indian Ocean: an assessment. *Int J Oceanogr* doi:10.1155/2011/983561.
- Singh A, Ramesh R (2015) Environmental controls on new and primary production in the northern Indian Ocean. *Prog Oceanogr* 131: 138-145.
- Singh A, Gandhi N, Ramesh R, Prakash S (2015) Role of cyclonic eddy in enhancing primary and new production in the Bay of Bengal. *J Sea Res* 97: 5-13.
- Smitha A, Rao KH, Sengupta D (2006) Effect of May 2003 tropical cyclone on physical and biological processes in the Bay of Bengal. *Int J Remote Sens* 27: 5301-5314.
- Strickland JDH, Parsons TR (1972) *A Practical Handbook of Seawater Analysis*. 2nd ed. Canada: Bulletin of Fisheries Research Board, 310 pages.

- Sournia A (1994) Pelagic biogeography and fronts. *Prog Oceanogr* 34: 109–120.
- Stuart V, Verheye HM (1991) Diel migration and feeding patterns of the chaetognath, *Sagitta friderici*, off the west coast of South Africa. *J Mar Res* 49: 493-515.
- Subramanian V (1993) Sediment load of Indian rivers. *Curr Sci* 64: 928–930.
- Swalethorp R, Malanski E, Agersted MD, Nielsen TG, Munk P (2015) Structuring of zooplankton and fish larvae assemblages in a freshwater-influenced Greenlandic fjord: influence from hydrography and prey availability. *J Plankton Res* 37: 102-119.
- Tian RC, Hu FX, Martin JM (1993) Summer nutrient fronts in the Changjiang (Yantze River) estuary. *Estuar Coast Shelf S* 37: 27-41.
- UNESCO (1994) Protocols for the joint global ocean flux study (JGOFS). Manual and Guides 29, 170 pages.
- Vinayachandran PN, Mathew S (2003) Phytoplankton bloom in the Bay of Bengal during the northeast monsoon and its intensification by cyclones, *Geophys Res Lett* 30: 1572, doi:10.1029/2002GL016717, 11.
- Vipin P, Sarkar K, Aparna SG et al (2015) Evolution and sub-surface characteristics of a sea-surface temperature filament and front in the northeastern Arabian Sea during November–December 2012. *J Mar Sys* 150: 1-11.
- Weikert H, John HC (1981) Experiences with a modified multiple opening closing plankton net. *J Plankton Res* 3: 167-177.

List of Figures

Figure 1. Sea surface salinity in the Bay of Bengal (a) based on the Levitus climatology, (b) based on the climatological data of the North Indian Ocean Atlas along a monthly scale, (c) variance in the sea surface salinity along each month.

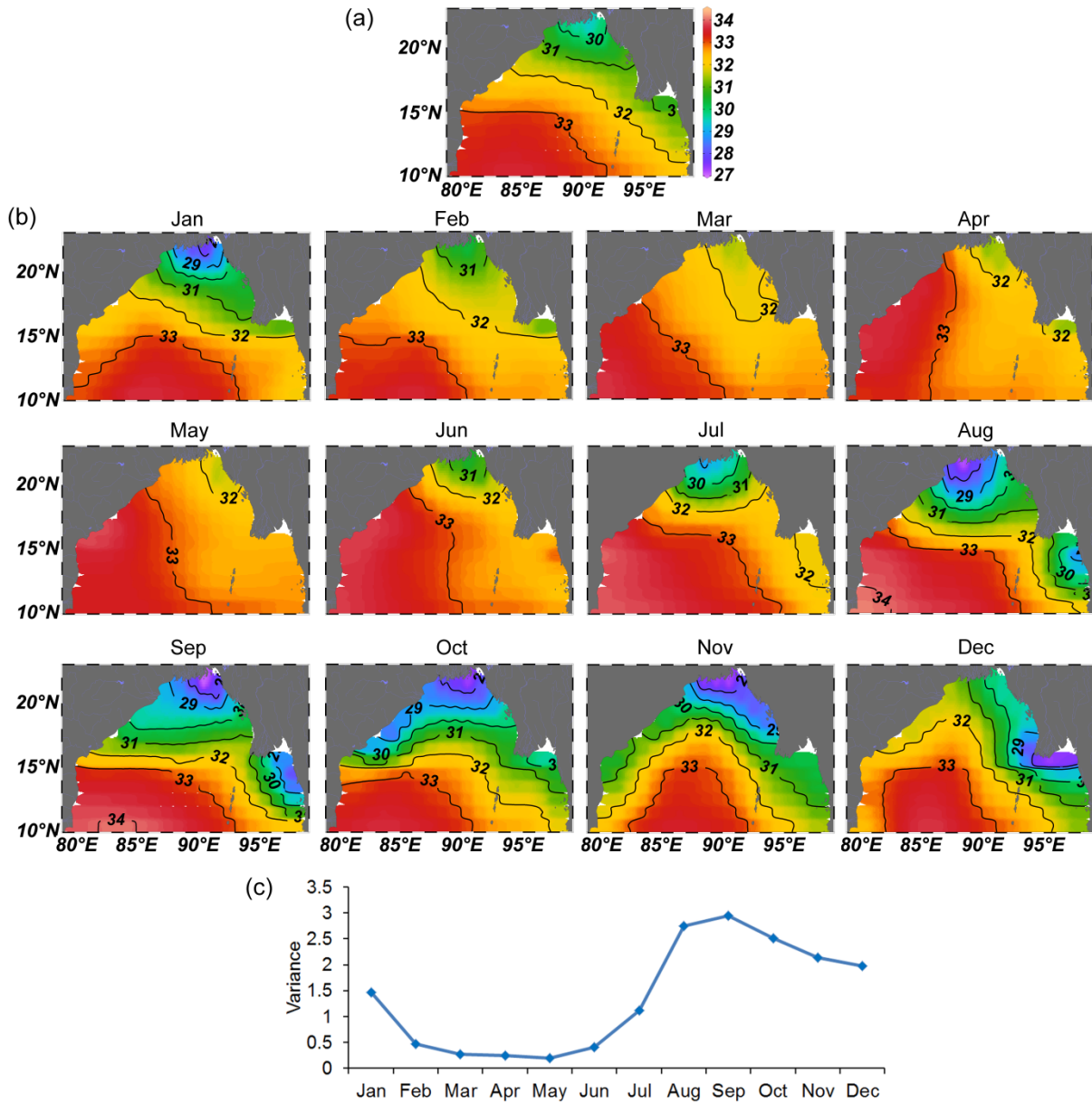


Figure 2. Distribution in the (a) station location, (b) salinity (psu), (c) potential density (kg m^{-3}), and (d) temperature ($^{\circ}\text{C}$) at the surface layer of Bay of Bengal. The frontal zones are encircled in white lines and also pointed out by arrows in the salinity diagram.

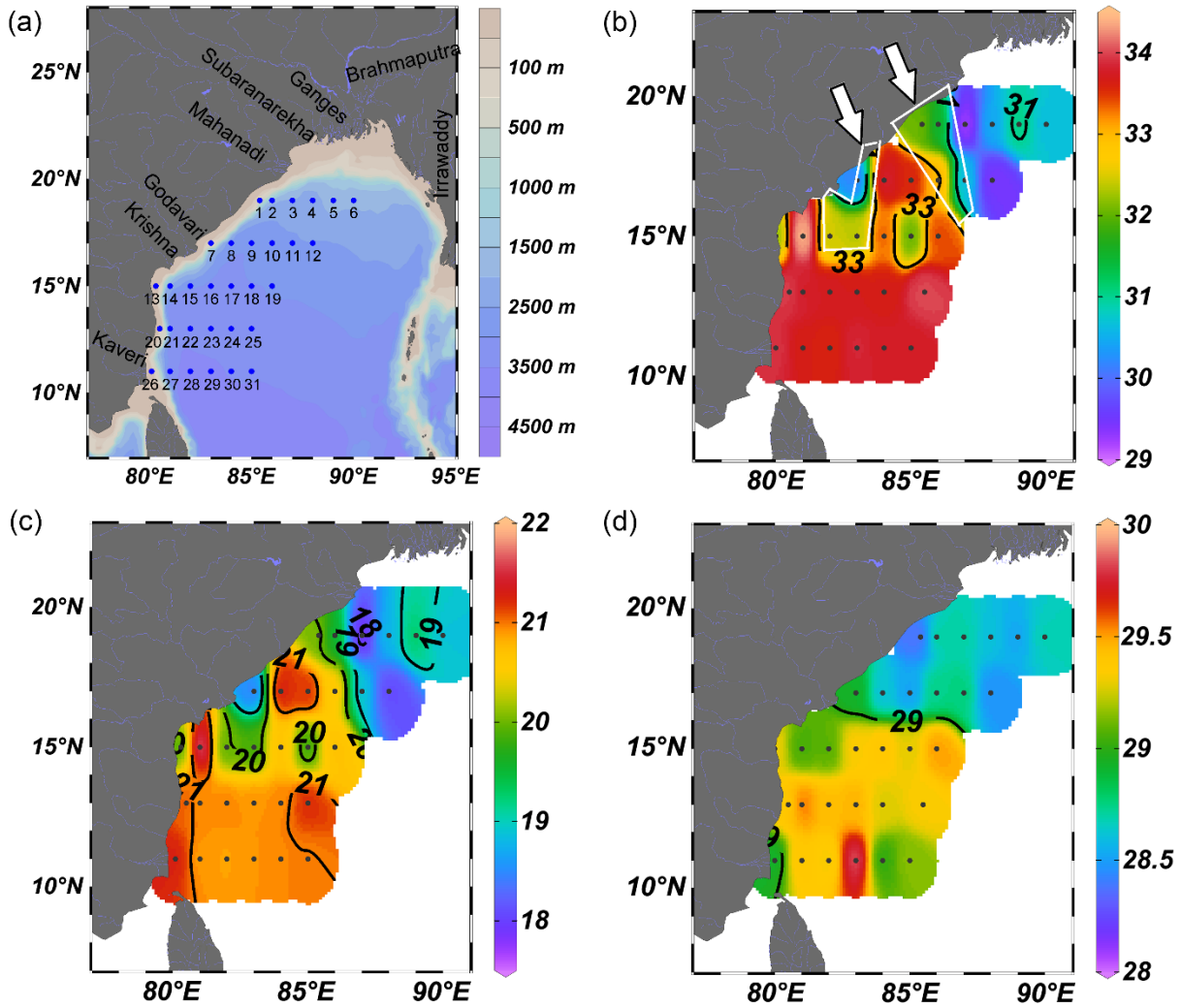


Figure 3. Vertical distribution of [a] salinity (psu), [b] potential density (kg m^{-3}) and [c] temperature ($^{\circ}\text{C}$) in the upper 150 m of the study area. Station locations are indicated by the arrows. The frontal regions are indicated by red arrows.

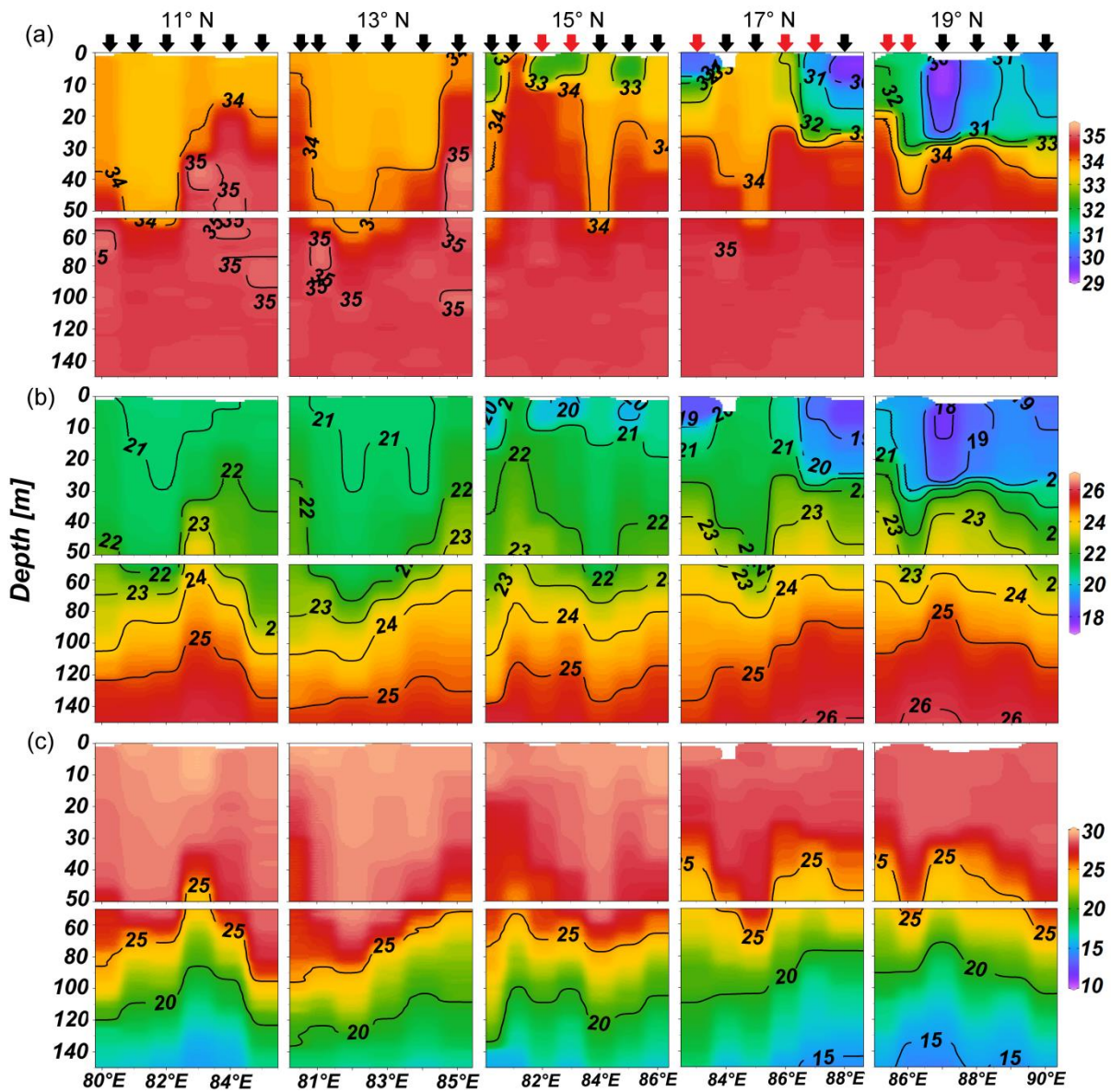
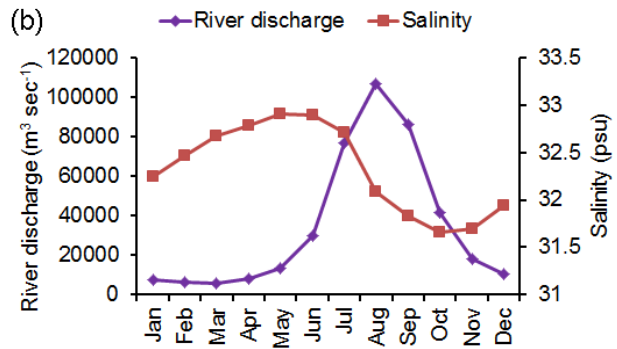
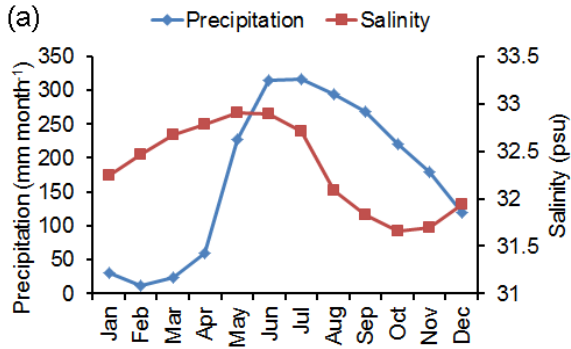


Figure 4. Monthly climatological data of (a) direct precipitation, and (b) river discharge in to the Bay of Bengal and (c) the annual discharge of the major rivers into the Bay of Bengal (excluding the Irrawadi River).



River	Annual discharge (m ³ sec ⁻¹)
Brahmaputra	19674
Brahmani	4916
Cauveri	235
Damodar	302

River	Annual discharge (m ³ sec ⁻¹)
Ganges	8088
Godavari	3061
Krishna	1642
Mahanadi	1883

Figure 5. Vertical distribution of [a] pH and [b] dissolved oxygen (ml l^{-1}) in the upper 150 m of the study area. Station locations are indicated by the arrows. The frontal regions are indicated by red arrows.

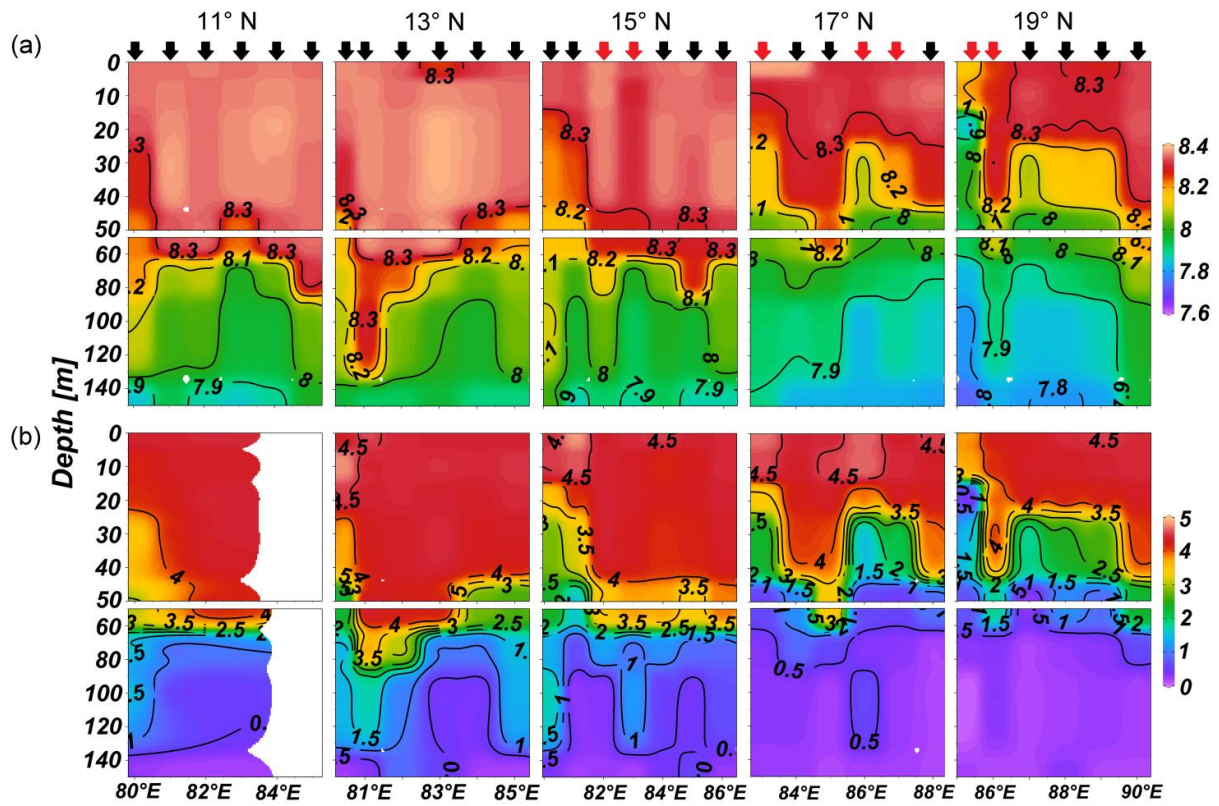


Figure 6. Vertical distribution of [a] nitrate (μM), [b] phosphate (μM) and [c] silicate (μM) in the upper 150 m of the study area. The station locations are indicated by the arrows. The frontal regions are indicated by red arrows.

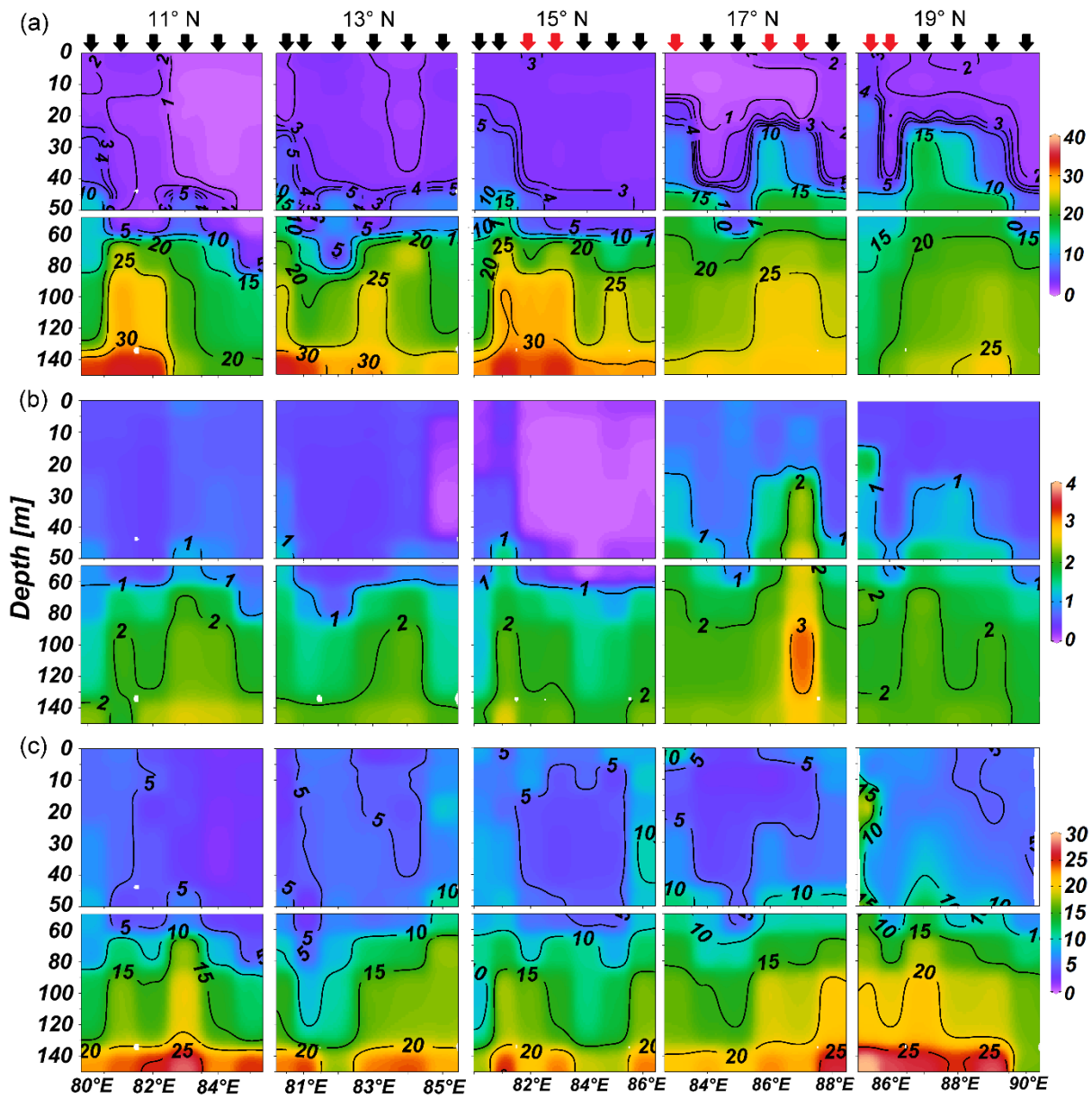


Figure 7. Vertical profile of the mean values of [a] chlorophyll *a* (mg m^{-3}), and [b] primary production ($\text{mg C m}^{-3} \text{ day}^{-1}$) in the frontal and non-frontal region, and distribution of [c] surface chlorophyll *a* (mg m^{-3}), [d] integrated column chlorophyll *a* (mg m^{-2}), [e] surface primary production ($\text{mg C m}^{-3} \text{ day}^{-1}$), [f] integrated column primary production ($\text{mg C m}^{-2} \text{ day}^{-1}$), [g] integrated mesozooplankton biomass (mL m^{-3}), and [h] integrated mesozooplankton abundance (ind m^{-3}) of MLD and TC in the Bay of Bengal. The frontal regions are indicated by red dots.

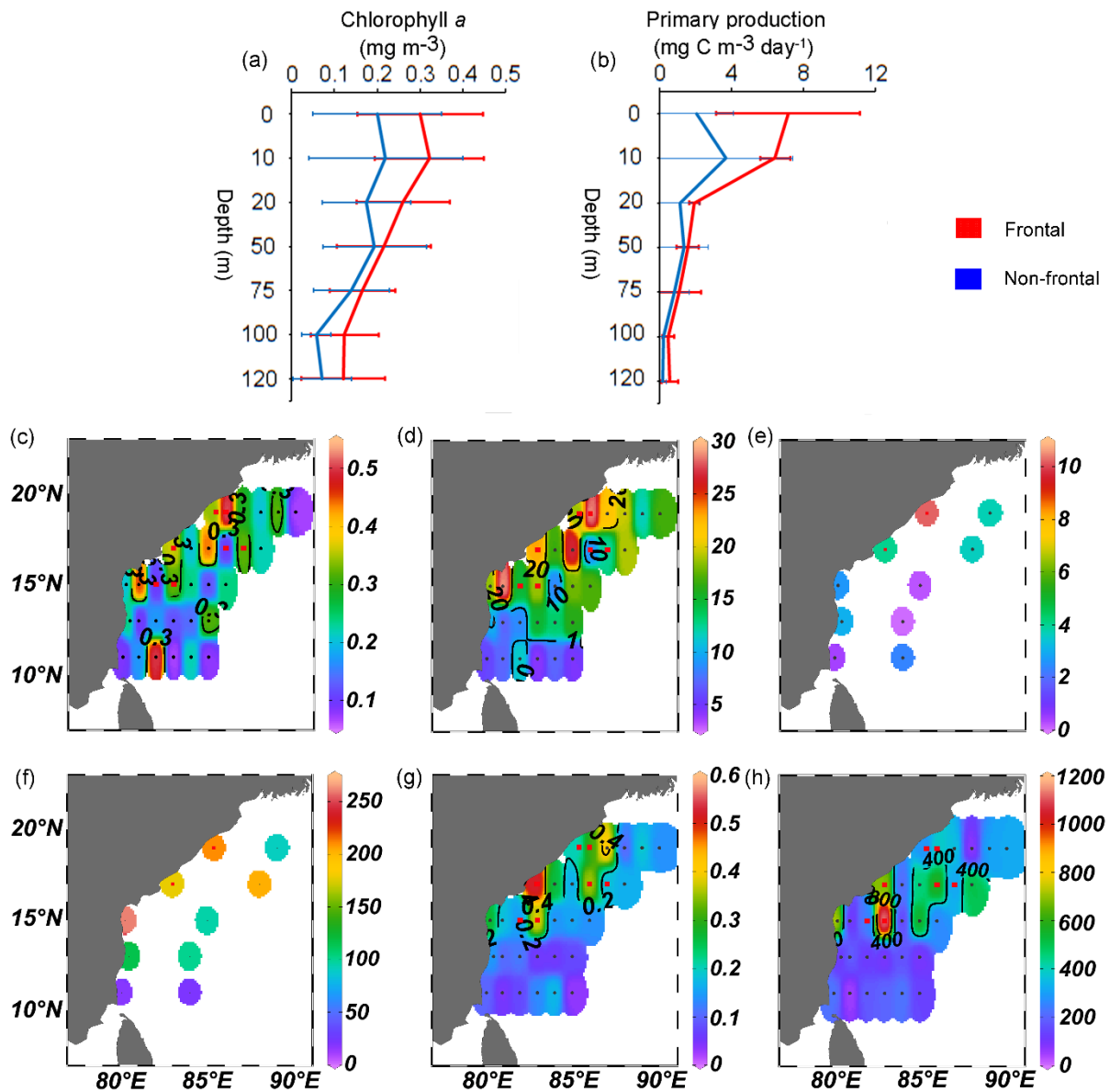


Figure 8. Diurnal ratio (night / day) in the abundance of the zooplankton taxa in the (a) frontal and (b) non-frontal regions. Only the taxa which were present in both day and night periods in both frontal and non-frontal regions were plotted.

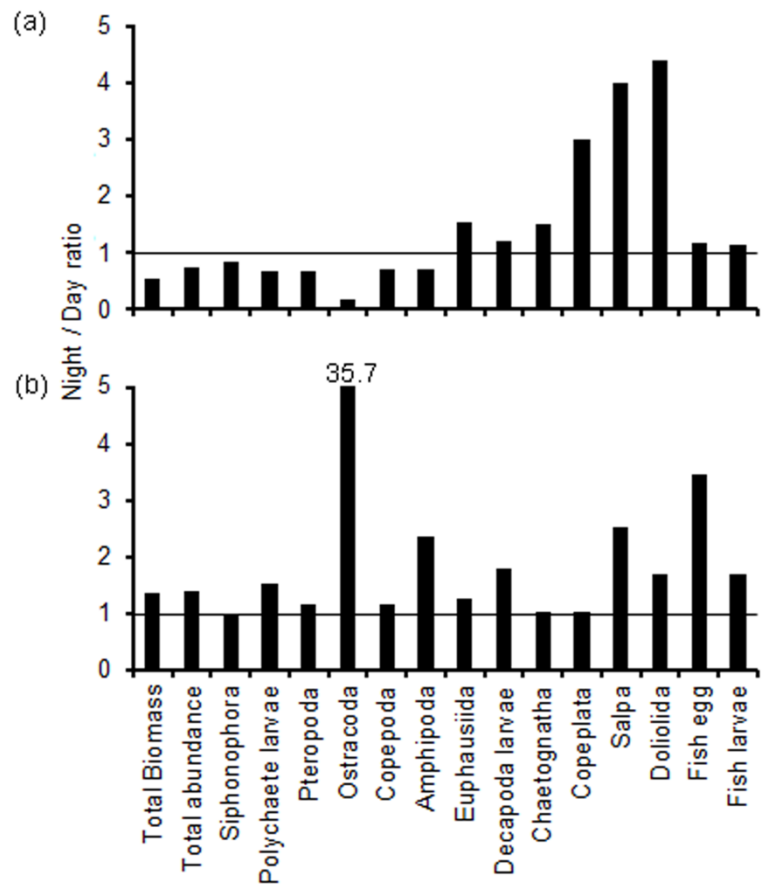


Figure 9. Canonical analysis of principal coordinates (CAP) based on the abundance of different zooplankton taxa.

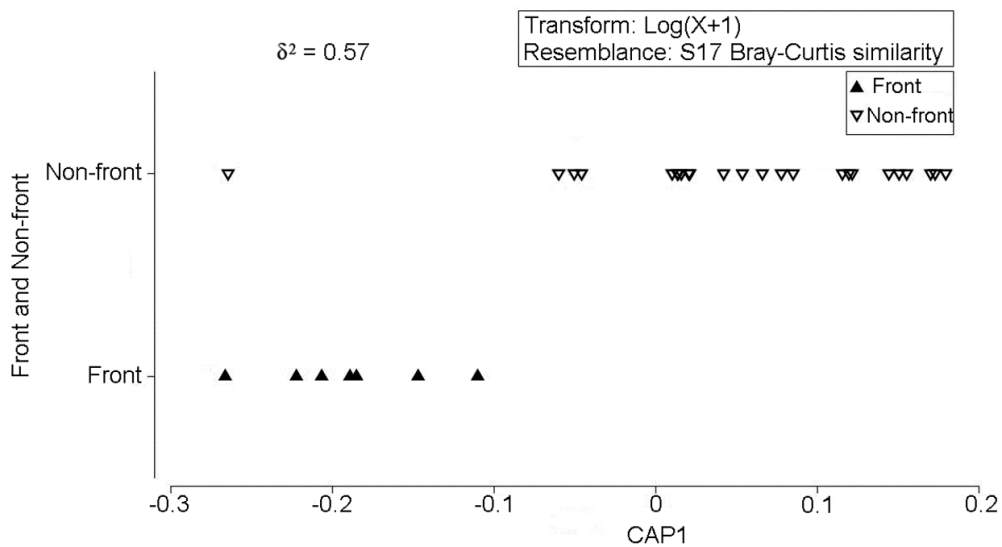


Figure 10. Result of the quadratic regression analysis between salinity and abundance of various zooplankton taxa. The taxa which were present in > 50% of the sampling locations and contributed > 0.01% of the total zooplankton population were only selected for the analysis (SIP – Siphonophora, MED – Medusa, CHA – Chaetognatha, DEC – Decapoda larvae, COP – Copepoda, AMP – Amphipoda, EUP – Euphausiid, MYS – Mysida, OST – Ostracoda, FOR – Foraminifera, SAL – Salpa, DOL – Doliolida, PTE – Pteropoda, THE – Heteropoda, GAS – Gastropoda larvae, POL – Polychaeta larvae, FE – Fish egg, FL – Fish larvae, COPL – Copelata, AMPH - Amphioxus) The statistically significant correlation coefficient (r) values are marked with an asterisk.

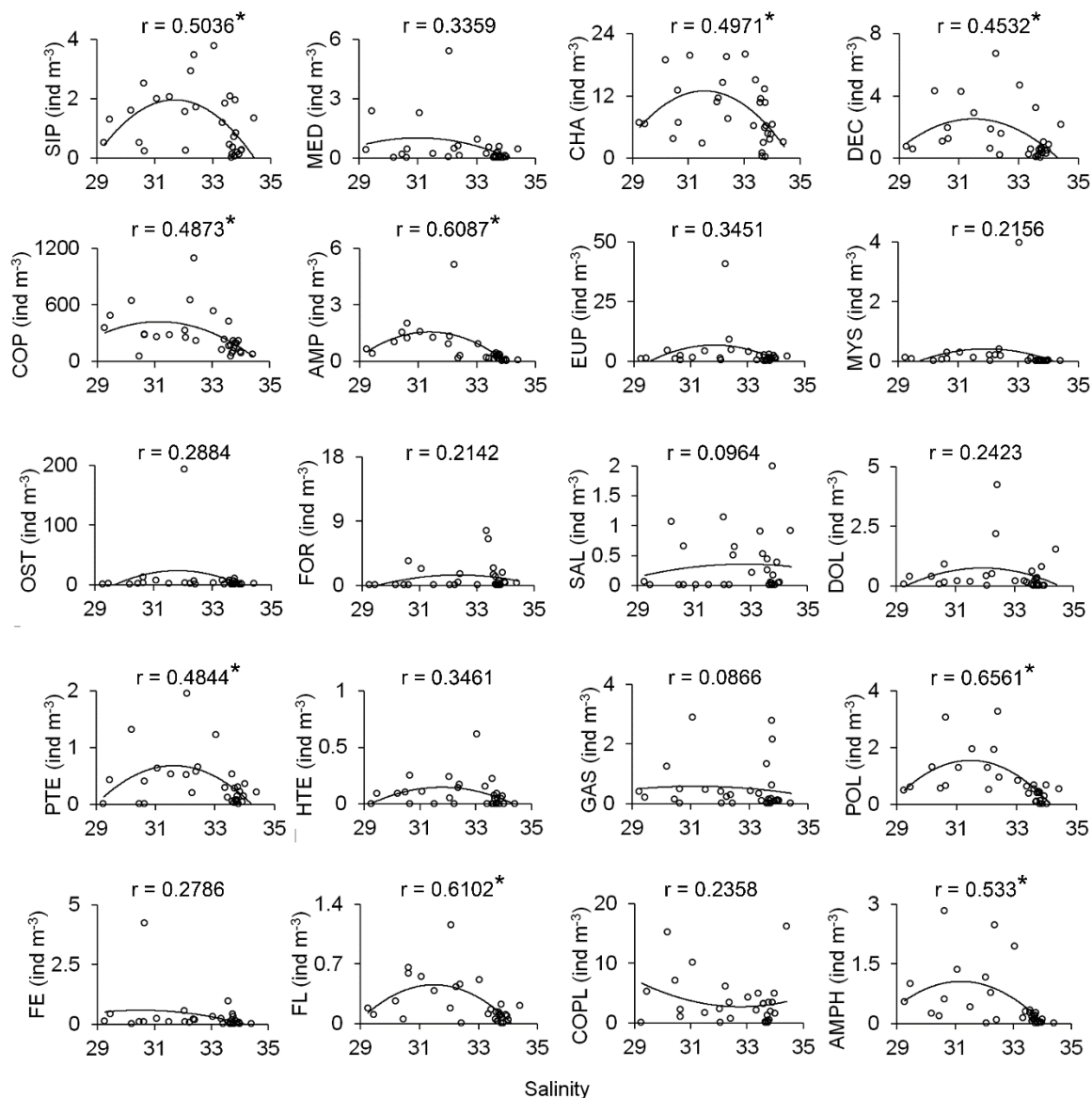


Table 1: Previous major reports on the physical processes controlling the biotic production in the Bay of Bengal during different seasons. (“+ve” and “-ve” indicated that the respective controlling factors had positive and negative influence on the plankton community, respectively).

Season	Major controlling factors	Impact	Source
Summer monsoon	Upwelling + Cold-core eddies	+ve	Muraleedharan et al. 2007
Summer monsoon	Upwelling + Mini-cold pool	+ve	Rao et al. 2006a
Summer monsoon	Warm gyres	-ve	Muraleedharan et al. 2007
Summer monsoon	Cold-core eddies	+ve	Prasanna Kumar et al. 2004
Inter monsoon	Cold-core eddies	+ve	Gomes et al. 2000 Prasanna Kumar et al. 2007 Fernandes 2008
Inter monsoon	Cyclone	+ve	Madhu et al. 2002 Rao et al. 2006b Smitha et al. 2006 Maneesha et al. 2011
Winter monsoon	Upwelling + Cyclone	+ve	Vinayachandran & Mathew 2003 Singh et al. 2015

Table 2: The abundance (integrated value for mixed layer depth and thermocline) of zooplankton taxa in the frontal (n = 7) and non-frontal zones (n = 24) of Bay of Bengal (abundance \pm std. deviation, unit - ind m⁻³). The ‘p’ value indicates the result of the t-test using the abundance of zooplankton taxa between the frontal and non-frontal locations. The ‘*’ indicates the statistically significant values (alpha = 0.05)

Fronts	Fronts	Non-fronts	Front / Non-front
Copepoda* (p = 0.0049)	468 \pm 318	212 \pm 147	2.21
Foraminifera (p = 0.5)	0.75 \pm 1.3	1.72 \pm 3.7	0.44
Medusa (p = 0.152)	1.03 \pm 1.9	0.37 \pm 0.6	2.78
Siphonophora* (p = 0.002)	2.2 \pm 1.2	0.86 \pm 0.8	2.56
Anthozoa	0	<0.01	0
Ctenophora	0	0.01 \pm 0.02	0
Polychaeta larvae* (p < 0.001)	1.7 \pm 1.1	0.51 \pm 0.5	3.33
Pteropoda* (p < 0.001)	0.9 \pm 0.6	0.21 \pm 0.2	4.29
Heteropoda (p = 0.3184)	0.15 \pm 0.2	0.06 \pm 0.08	2.5
Gastropoda larvae (p = 0.5774)	0.34 \pm 0.4	0.53 \pm 0.9	0.64
Cephalopoda* (p = 0.024)	0.1 \pm 0.1	0.03 \pm 0.05	3.33
Ostracoda (p = 0.555)	2 \pm 1.7	11 \pm 39	0.18
Amphipoda (p = 0.093)	0.87 \pm 0.5	0.64 \pm 1.1	1.36
Euphausiida* (p = 0.0076)	4.14 \pm 2.6	2.79 \pm 8.1	1.48
Decapoda larvae* (p = 0.0316)	2.5 \pm 1.6	1.13 \pm 1.6	2.21
Stomatopoda (p = 0.7064)	0.01 \pm 0.02	0.01 \pm 0.02	1
Chaetognatha* (p = 0.0355)	13.3 \pm 6.6	7.29 \pm 4.5	1.82
Copelata (p = 0.7156)	3.93 \pm 5.2	3.28 \pm 3.8	1.2
Pyrosoma	0	0.34 \pm 1.5	0
Salpa (p = 0.887)	0.35 \pm 0.4	0.32 \pm 0.5	1.09
Doliolida* (p = 0.011)	1.15 \pm 1.5	0.25 \pm 0.4	4.6
Fish egg (p = 0.533)	0.13 \pm 0.1	0.34 \pm 0.9	0.38
Fish larvae* (p = 0.002)	0.5 \pm 0.3	0.15 \pm 0.2	3.33
Mysida* (p = 0.031)	0.71 \pm 1.4	0.05 \pm 0.1	14.2
Amphioxus* (p = 0.007)	1.14 \pm 1.2	0.33 \pm 0.4	3.45

Table 3: Result of the Bio-Env analysis (Corr. – correlation)

No. Variables	Corr.	Selections
3	0.25	DO (ml l ⁻¹), nitrate (μM), potential density (kg m ⁻³)
3	0.24	DO (ml l ⁻¹), nitrate (μM), salinity
2	0.24	DO (ml l ⁻¹), nitrate (μM),